journal

J. Am. Ceram. Soc., 82 [4] 953–60 (1999)

Tribooxidational Effects on Friction and Wear Behavior of Silicon Nitride/Tool Steel and Silicon Nitride/Gray Cast Iron Contacts

José R. Gomes and António S. Miranda

Department of Mechanical Engineering, University of Minho, 4810 Guimarães, Portugal

Rui F. Silva* and Joaquim M. Vieira

Department of Ceramics and Glass Engineering, UIMC, University of Aveiro, 3810 Aveiro, Portugal

Unlubricated pin-on-disk wear tests of Si_3N_4 against tool steel and gray cast iron were performed at 5 N of normal load, 0.5 m/s of sliding speed, and environmental temperature in the range 22°–600°C. The friction coefficient of Si_3N_4 sliding against tool steel and gray cast iron had maximum values of 0.88–0.98 for tests at 100°C. The friction coefficient of Si_3N_4 sliding against gray cast iron couples had minimum values of 0.48–0.57 at 400°C. Because of the increased third-body protection, the wear coefficient of the Si_3N_4 pins of the Si_3N_4/gray cast iron couples decreased by 1 order of magnitude from 1.6×10^{-5} mm^3/(N·m) at room temperature to 1.3×10^{-6} mm^3/(N·m) at 600°C. Fe_2O_3 and Fe_3O_4 resulting from tribooxidation of the metallic disks were the main constituents of the wear debris and adherent tribolayers. Activation energy values (6.3–13.7 kJ/mol) were comparable to those of oxidation wear of steel (7.3–11.8 kJ/mol) but were much lower than the activation energy for oxidation of iron alloys in static conditions. Calculations of the activation energy of the oxidation wear corroborate the morphological observations of a sacrificial action of the metallic surface protecting the ceramic material.

I. Introduction

ADVANCED CERAMICS are successfully used in a wide variety of engineering applications as triboelements involving contacts with metallic surfaces, such as drawing dies, roller bearings, automotive or aerospace engine parts, and power generation system components.[1–5] Si_3N_4-based ceramics are high-performance materials for such applications. Si_3N_4 materials have lower density and thermal expansion than metals, and their mechanical stability and corrosion resistance over a wide range of temperatures are superior to those of several other high-strength ceramic materials.[3,5,6]

Detailed information about the friction and wear behavior of any system is needed before its effective application as a successful tribosystem. Iron alloys, such as steel and cast iron, are the most common metallic materials for tribological applications. Although there are several studies on the tribology of Si_3N_4 sliding against these alloys at room temperature,[1,2,7–12] few studies have been performed on the effect of temperature.[13,14] Previous studies on tribological performance of Si_3N_4 against steel and cast iron at room temperature have shown that tribochemical reactions, plastic deformation, and microfracture control the interface dynamics. Intrinsic factors, such as porosity and intergranular phase volume, and extrinsic parameters, such as humidity, sliding speed, and contact load, determine the dominating wear mechanism.[2,7,12] The ceramic surface tends to be protected by a tribofilm of composite nature made of metal-oxidized debris and very fine ceramic wear particles.[7,9–11] The rheology and adhesion of this tribolayer become even more important for the ceramic wear resistance than the properties of the bulk material themselves.

The experimental study of ceramic/metal contacts sliding above room temperature bears directly on the performance of these contacts in specific high-temperature applications, such as the inlet and exhaust valves in internal combustion engines. Valves operate in a temperature range of 300° to 700°C, in aggressive environment conditions. Recent results show that the replacement of conventional metallic valves by Si_3N_4 valves results in significant improvements in valve wear life.[5] A lubricious action is afforded by the oxide films with a composite ceramic/metal nature that are formed at the sliding interface.[15] High-speed metal cutting, where temperature increases to 1200°C by frictional heating and chip deformation, also is an extreme contact condition.[15] Ceramic tools, similar to those made of Si_3N_4, either in bulk or in composite form, are unique materials to withstand such extreme thermomechanical loading.[15,16] High-temperature applications of ceramics necessarily exclude the use of conventional lubricants. Unlubricated sliding experiments have been increasingly required because of environmental concerns and legislation.[17] The experiments also are imperative in developing vacuum precision equipment.[4]

The high-temperature tribological behavior of Si_3N_4 materials was characterized using self-mated pairs; the general trend was increased ceramic wear with temperature.[6,18–22] Dong and Jahanmir[6] proposed wear with temperature diagrams showing that, at low temperatures in air, at very slow sliding speeds (0.0014 m/s), the effect of a hydroxylated silicon oxide film resulted in preservation of the ceramic surface and low friction coefficients ($f \approx 0.3$). Above 400°C and up to 900°C, the tribological behavior was dominated by the tribooxidation of the ceramic; the friction and the wear coefficients significantly increased with temperature. A transition to a severe wear regime controlled by microfracture of the ceramic occurred for contact loads between 10 and 20 N.

Significant differences in the tribological characteristics have been observed above room temperature when nitride ceramics slide on a different material, namely steels.[13,14] The ceramic wear coefficient (K) in Si_3N_4/steel contacts decreases almost 1 order of magnitude above 400°C, whereas it increases 2 orders of magnitude, up to catastrophic values of $K \approx 10^{-4}$ mm^3/(N·m), when Si_3N_4 is tested against itself.[14] The dependence of f on temperature also reveals distinct trends; i.e., it decreases from $f \approx 0.7$ at room temperature to $f \approx 0.4$ at 600°C for Si_3N_4/steel contacts, whereas it remains almost constant ($f \approx 0.7$) for self-mated pairs.[14] Protective layers transferred

R. O. Scattergood—contributing editor

Manuscript No. 190776. Received August 13, 1997; approved August 19, 1998.
*Member, American Ceramic Society.

Table I. Composition, Hot-Pressing Temperature, Intergranular Phase Volume, and Mechanical Properties of the Si_3N_4-Based Pin Materials†

Sample	Composition (mol%)				T (°C)	V_L (%)	H (GPa)	K_{Ic} (MPa·m$^{1/2}$)
	Si_3N_4	SiO_2	Ce_2O_3	AlN				
SN1	76.2	7.3	0.9	15.6	1500	10.1	19.7	4.1
SN2	73.2	7.5	1.8	17.5	1450	12.6	18.2	4.1
SN3	69.0	8.0	3.5	19.5	1450	16.9	17.9	3.5

†Raw materials: Si_3N_4, LC12, H. C. Starck, Inc., New York; CeO_2, grade puriss, Fluka Chemical Corp., Ronhonkoma, NY; AlN, grade C, H. C. Starck.

Table II. Composition and Hardness of the Metallic Disks

Material	Code	Composition	H (GPa)
Annealed tool steel (TS)	DIN 1.2080	2.0% C; 12% Cr	2.5
Gray cast iron (GCI)	Grade 200	3.9% C; 2.9% Si; 0.9% Mn; 0.04% (max) S; 0.1% (max) P	1.9

from the oxidized steel counterface inhibit the wear of the ceramic at high temperature.[13,14]

In the present work, unlubricated pin-on-disk experiments of Si_3N_4/iron alloy couples are performed in the range 22°–600°C. Tool steel and gray cast iron have been chosen as disk materials because of their distinct mechanical resistance at high temperature. The third-body protection of the ceramic surface by the increased extent of oxidized metal transfers with temperature is investigated. The tribooxidation process of both the metallic surface and wear debris is quantitatively discussed by calculating the activation energies of the wear coefficients. Recalculated data on the activation energy of wear of Si_3N_4/steel contacts from the literature[14] and published results for oxidation wear of steel[23–27] are compared.

II. Experiments and Materials

Ceramic pins of the system AlN–CeO_2–Si_3N_4 were tested against tool steel (TS) and gray cast iron (GCI) disks in a pin-on-disk tribometer. Tests were performed without lubrication at a sliding speed of 0.5 m/s with a constant normal force (F_n) of 5 N. For room-temperature experiments, an acrylic chamber isolated the rotating head and pin holder from the external environment. A relative humidity of 50% was kept constant inside the acrylic chamber. Experiments above room temperature and up to 400°C were accomplished using an electric air blower. A propane burner replaced the air heater for temperatures in the range 500°–600°C. An infrared pyrometer and a digital controller regulated the electric power, the gas flow of the air heater and the burner, and the test temperature at the disk surface.

A data acquisition system was used to record at regular periods of time the frictional force (F_f) that was accessed by a bend-type loading cell. f was calculated from the average values of F_f as $f = F_f/F_n$. Tests were regularly stopped at the end of each 3 km run to measure the pin weight loss. Total sliding distances ranged from 9 to 15 km. Disk wear volume was evaluated by profilometry. After an initial running-in period, the wear coefficient (K) was calculated as $K = V/(F_n x)$, where V is the wear volume and x the sliding distance. Average values and standard deviation values of f and K were calculated from the set of measurements obtained from the single runs.

Ceramic pins were machined from disks that had been hot-pressed at 30 MPa of applied pressure for 60 min of dwell time at isothermal temperatures given in Table I. The pins had a conical geometry with a flat end of 1 mm initial diameter. Three Si_3N_4 batches with distinct values of chemical composition of sintering aids and intergranular phase volume were tested. The chemical composition, glass-phase volume fraction, hardness, and toughness of batches SN1–SN3 are given in Table I. Volume fractions of the intergranular glassy phase (V_L) are representative of low (SN1), medium (SN2), and high (SN3) additive content batches. V_L values were calculated from the amount and composition of the sintering aids, using the density of glasses of similar composition.[28] Hardness (H) was measured using a Vickers indenter with a load of 9.8 N and taking the average from 20 indentations for each sample. Fracture toughness (K_{Ic}) was determined from crack lengths at indentation corners, according to Niihara's equation.[29]

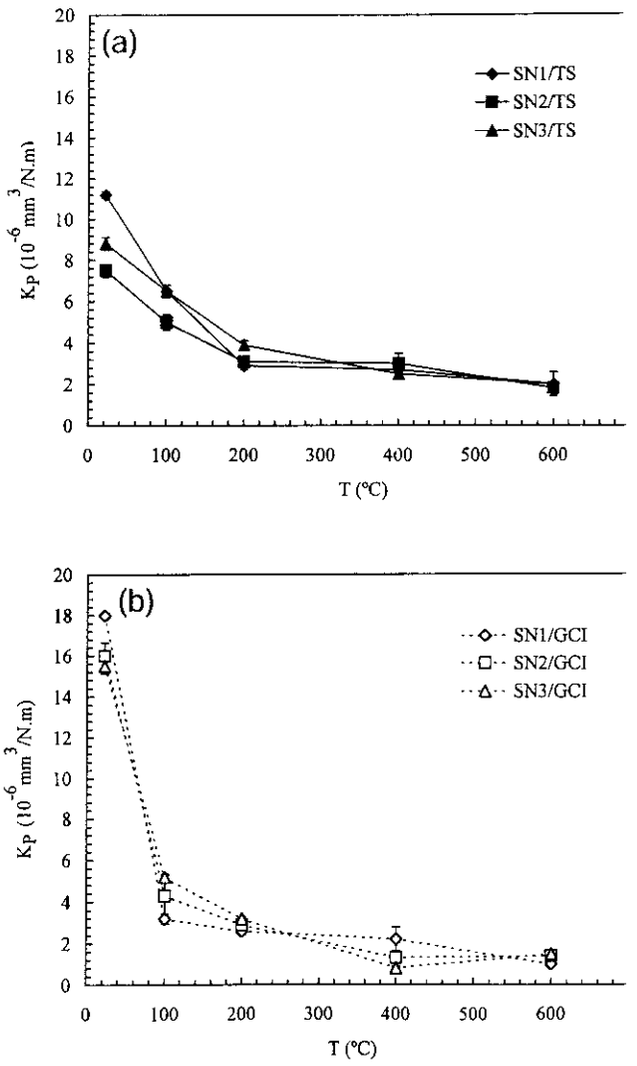

Fig. 1. Effect of ambient temperature on the wear coefficient (K_P) of three grades (SN) of Si_3N_4 pins tested against: (a) tool steel (TS) and (b) gray cast iron (GCI). F_n = 5 N; v = 0.5 m/s.

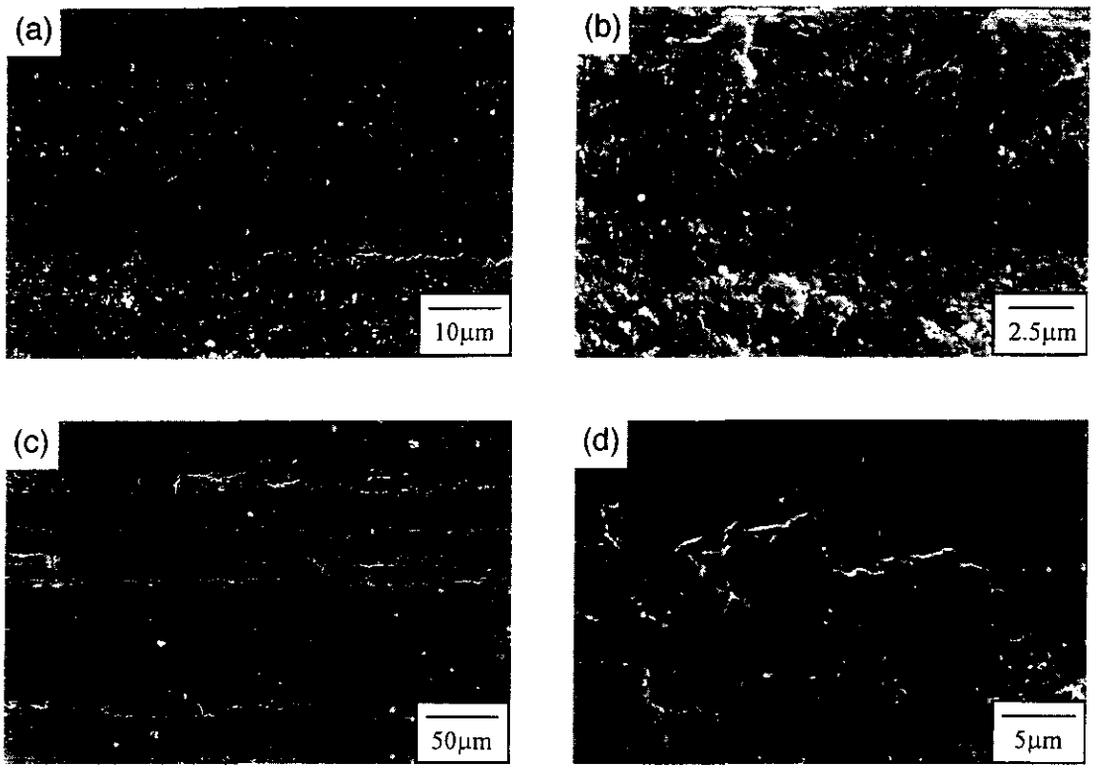

Fig. 2. SEM/SE images of Si_3N_4 pin worn surfaces tested against tool steel at different temperatures: (a) room temperature; (b) 100°C; (c) 600°C; and (d) 600°C, high magnification. Sliding direction of the opposite surface is from left to right.

Tool steel and gray cast iron were the counterface disk materials. Composition and properties of the two alloys are given in Table II. The surfaces of the disks were polished with 800 grit silicon carbide paper followed by finishing with 1 μm diamond paste, ultrasonically cleaned, and degreased with ethanol. The final surface roughness, as measured by profilometry, was 0.05 and 0.3 μm R_a for the tool steel disk and the cast iron disk, respectively.

Chemical and morphological characterization of the worn surfaces of the pins, the track surfaces of the disks, and the wear debris were performed using scanning electron microscopy (SEM) with chemical analysis (EDS) at the end of the tests. The amorphous or the crystalline nature of the wear debris was characterized by X-ray diffractometry (XRD) analysis.

III. Results

(1) Si_3N_4/Tool Steel Tribopairs

Figure 1 gives the pin-wear coefficients (K_P) at $v = 0.5$ m/s in the temperature range 22°–600°C for the SN/TS and SN/GCI sliding pairs. When tool steel is used as the sliding disk, the pin-wear coefficients decrease from room temperature to 600°C (Fig. 1(a)). The decrease is steep in the 22°–200°C range, with similar behavior for the three ceramic grades. The final surface morphology of the ceramic pins is illustrated in Fig. 2. All micrographs in this study are aligned in such way that the sliding direction of the opposite surface is from left to right. The morphology of the worn surfaces of the SN1 grade can be described as follows: (i) at room temperature, the SN surfaces have a polished appearance (Fig. 2(a)) and are almost free of adherent debris; (ii) at intermediate temperatures, 100° and 200°C, an incoherent (not aggregated) layer of wear debris is observed on the ceramic surfaces (Fig. 2(b)); (iii) from 400° to 600°C, a tribofilm spreads along the worn surfaces in the sliding direction (Fig. 2(c)), with a coherent appearance, as shown under high-magnification (Fig. 2(d)). EDS analysis of the debris-free region inside the wear track of the pin of the SN1/TS tests at 600°C reveals the ceramic elements silicon, aluminum, and cerium and small traces of iron from the metal (Fig. 3(a)). If the same analysis is made on the tribolayer (Fig. 3(b)), the intensity of the oxygen, iron, and chromium peaks reveals that it is rich in metallic oxides from the disk.

Disk wear coefficients (K_D) at $v = 0.5$ m/s in the temperature range 22°–600°C for the SN/TS and SN/GCI sliding pairs are given in Fig. 4. K_D values are higher than K_P values for all temperature conditions except at room temperature (Figs. 1 and 4). The values of K_D for tool steel have a steep increase when the test temperature increases to 100°C (Fig. 4(a)). Above

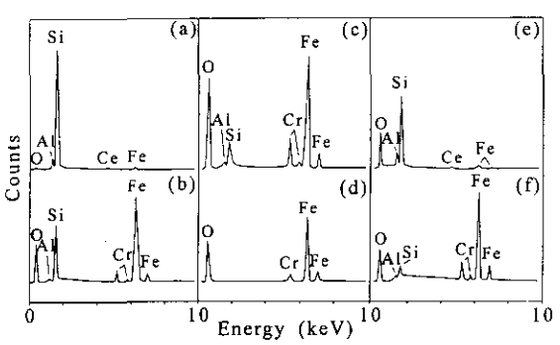

Fig. 3. SEM/EDS spectra of SN/TS worn surfaces and wear debris: (a) debris-free region on the worn surface of the Si_3N_4 pin after sliding against tool steel at 600°C; (b) adhering tribolayer on the worn surface of the same pin as (a); (c) adhering tribolayer inside the wear track of the tool steel disk at 400°C; (d) the bottom of a delaminated region taken from inside of the same wear track as (c); (e) loose wear debris from pairs tested at room temperature; and (f) loose wear debris from pairs tested at 600°C.

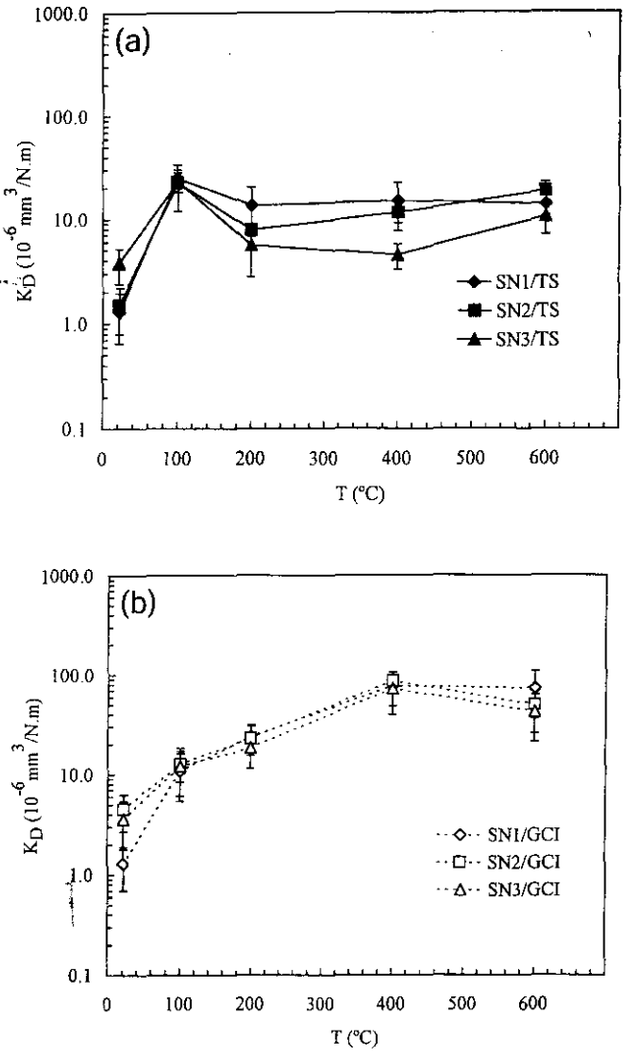

Fig. 4. Effect of environmental temperature on the wear coefficient of the metallic disks (K_D) tested against Si_3N_4 pins (SN): (a) tool steel (TS) disks and (b) gray cast iron (GCI) disks.

100°C, K_D becomes almost independent of temperature. Representative cases of disk track morphology are shown in Fig. 5. Figure 5(a) shows many wear grooves on the metal surfaces at room temperature. When the temperature increases, the disk surfaces oxidize, and a covering layer with a metal/ceramic composite nature is formed (Fig. 5(b)), as illustrated by the presence of iron, silicon, and oxygen in the EDS spectra (Fig. 3(c)). Film delamination (Fig. 5(b)) exposes a silicon-free and oxidized subsurface layer (Fig. 3(d)), revealing that silicon contamination from the ceramic counterface abruptly decreases in depth. In general, EDS spectra of disk tracks show an outer contamination of silicon (Fig. 5(a)), but the iron oxide nature of the layer is essentially denoted by spectra taken from delaminated cavities (Fig. 5(b)).

Figure 6 presents the f values for individual tests conducted from 22° to 600°C. For SN/TS experiments, an increase of f from room temperature to 100°C is observed, followed by a slow decrease from an average value of $f = 0.94$ at 100°C to $f = 0.76$ at 600°C. f is almost constant during the tests at room temperature in the absence of adherent material. The increasing spread of the wear debris with temperature, already discussed, is revealed by the characteristic stick-and-slip effect in the time profile of F_f, mainly at 400°–600°C. F_f profiles have increasingly oscillating values at high test temperatures. Fluctuations of f result from the intermittent destruction and renewal of the adherent wear-debris layer.[30,31] Peaks are observed when the agglomeration of the wear particles reaches a maximum volume, thus requiring higher frictional forces. The collapse of this layer due to the lack of cohesion results in the subsequent decrease of f.[32]

(2) *Si_3N_4/Gray Cast Iron Tribopairs*

The decrease of K_P for SN/GCI contacts above room temperature is even more abrupt than for Si_3N_4 against tool steel. K_P decreases by 1 order of magnitude at 100°C (Fig. 1(b)). The ceramic worn surfaces of the SN/GCI contacts reveal morphological features similar to the ones described for the SN/TS tribopairs: (i) the ceramic surfaces at room temperature are polished, with a smooth appearance (Fig. 7(a)); (ii) above room temperature, the Si_3N_4 surfaces are covered by thick protective iron-rich transfers from the disk surface (Figs. 7(b)–(d)). The tribolayers are less aggregated at the intermediate temperatures (100°–200°C) (Fig. 7(b)) than at the higher temperatures (400°–600°C) (Figs. 7(c) and (d)).

The wear rate of the gray cast iron is strongly dependent on temperature, from 22° to 400°C (Fig. 4(b)). Tool steel and gray cast iron show a similar wear behavior when tests are performed in the range 22°–100°C, but a very pronounced difference is noted above 200°C (Fig. 4). The gray cast iron disks are severely worn, by 1 order of magnitude more than the tool steel disks. The wear tracks of gray cast iron show a flat appearance after room-temperature tests; the surfaces appear as if they had been lapped (Fig. 8(a)). As temperature increases, the graphite flake cavities tend to close by material displacement in the sliding direction (Fig. 8(b)). At 600°C, the delamination of the oxidized gray cast iron surfaces is very pronounced (Fig. 8(c)), and EDS analysis gives spectra with trends similar to those presented in Figs. 3(c) and (d). A steep increase of f in SN/GCI couples is observed from room temperature to 100°C (Fig. 6). A marked decrease of f occurs when the temperature further increases from 100° to 400°C.

The tribological behavior of Si_3N_4/iron alloy sliding couples

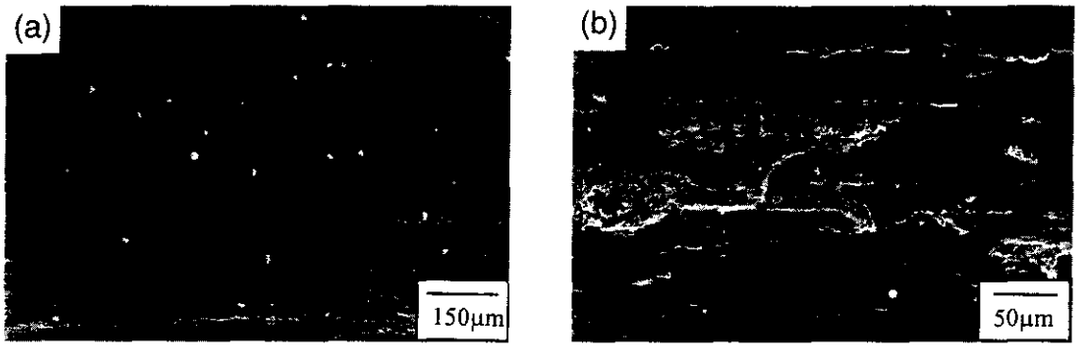

Fig. 5. SEM/SE images of tool steel disk tracks after sliding at (a) room temperature and (b) 400°C. Sliding direction of opposite surface is from left to right.

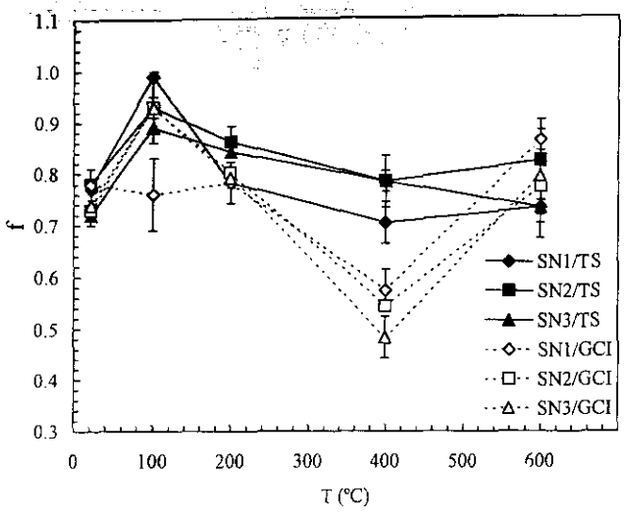

Fig. 6. Effect of temperature on f of SN/TS and SN/GCI sliding experiments.

at room temperature has been discussed in a previous paper.[7] As a result of graphite pulling out of the gray cast iron wear surfaces, the Si_3N_4 wear coefficient of the SN/GCI couples is higher than that of the SN/TS couples, because the gray cast iron wear surface is rougher than that of the tool steel. On the contrary, in the presence of a tribolayer that develops for temperatures above 100°C, K_P of the SN/GCI couples levels off with the values of K_P of the SN/TS (Figs. 1(a) and (b)). Also, high sliding speeds at room temperature develop the tribolayer and bring to coincidence the values of K_P of both systems.[7]

The effect of the amount of V_L on the wear behavior at room temperature also has been investigated in the quoted work.[7] K_P decreases with increasing V_L for test conditions of low sliding speed, where the ceramic surfaces are almost free of adhering debris. Adhesion of the tribolayer to the Si_3N_4 surface is improved by the reactivity of the wear debris toward the glassy phase. The fractional area of the glassy phase on the Si_3N_4 surface is proportional to V_L. Whenever the ceramic surface tends to become partially coated as temperature or sliding speed increases, or in dry atmospheres, the effect of V_L, on the contrary, vanishes. That explains why the results above room temperature are very similar to the samples of all three Si_3N_4 grades.

(3) Analysis of Wear Debris

Representative morphologies of the loose wear debris for 22° and 600°C tests are shown in Fig. 9. The given examples, taken from SN3/TS contacts, are characteristic of the wear debris resulting from the nitride contacts against both iron alloys: (i) at room temperature, the loose wear debris consists of a combination of large plates (~15 μm) and fine particles (Fig. 9(a)); (ii) as the temperature increases, the proportion of small particles with a rounded appearance prevails (Fig. 9(b)).

EDS spectra of the wear debris of tests at 22°C reveal the presence of elements from the ceramic pin (silicon, aluminum, and cerium) with a smaller proportion of iron from the metallic disk (Fig. 3(e)). In contrast, in the EDS spectra corresponding to the tests performed at 600°C, iron and chromium dominate over the silicon and aluminum from the ceramic pin (Fig. 3(f)). Oxygen peaks are very intensive in both spectra. These observations are corroborated by XRD analysis according to powder diffraction files:[33] (i) at room temperature, the wear debris is composed of amorphous silica and ferrite (Card No. 6-696) with traces of α-Si_3N_4 (Card No. 41-360); (ii) at 600°C, the wear debris is of crystalline nature, composed of rhombohedral oxide α-Fe_2O_3 (Card No. 24-72) and of spinel oxide Fe_3O_4 (Card No. 11-614).

IV. Discussion

The wear behavior of the Si_3N_4 ceramic pins in sliding against gray cast iron and tool steel is controlled by the protection afforded by the oxidized iron-rich tribofilm. As temperature increases above 400°C, the tribofilm becomes a coherent and extensive layer that grows on the ceramic pin

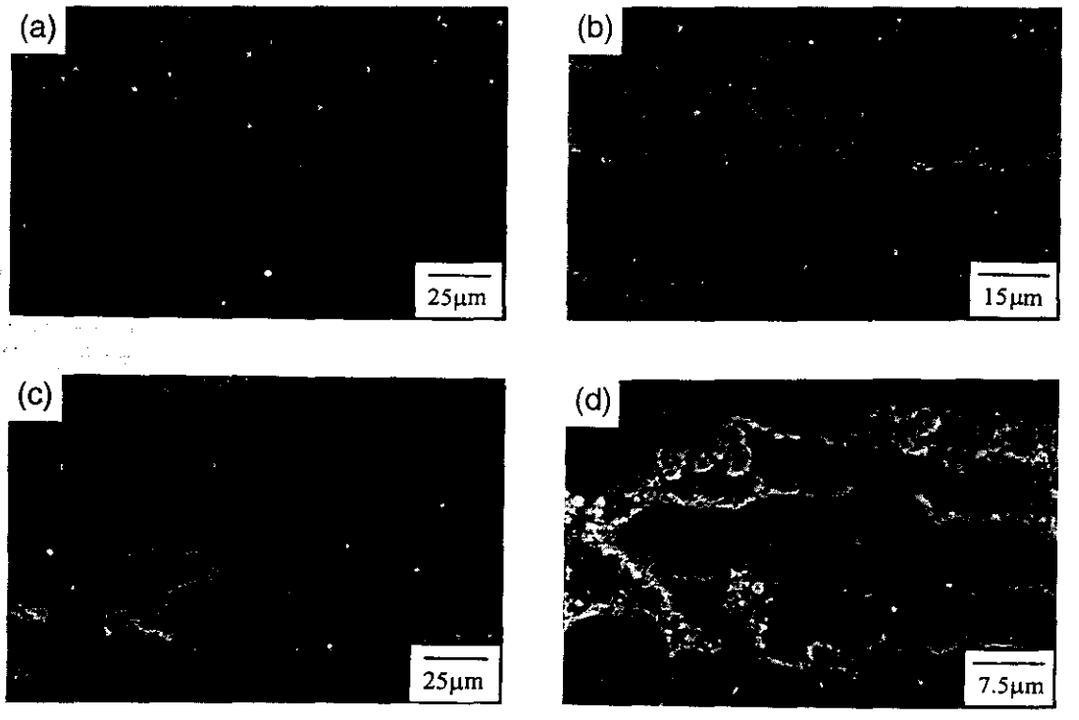

Fig. 7. SEM/SE images of the worn surfaces of Si_3N_4 pins tested against gray cast iron at different temperatures: (a) room temperature; (b) 100°C; (c) 600°C; and (d) 600°C, high magnification. Sliding direction of opposite surface is from left to right.

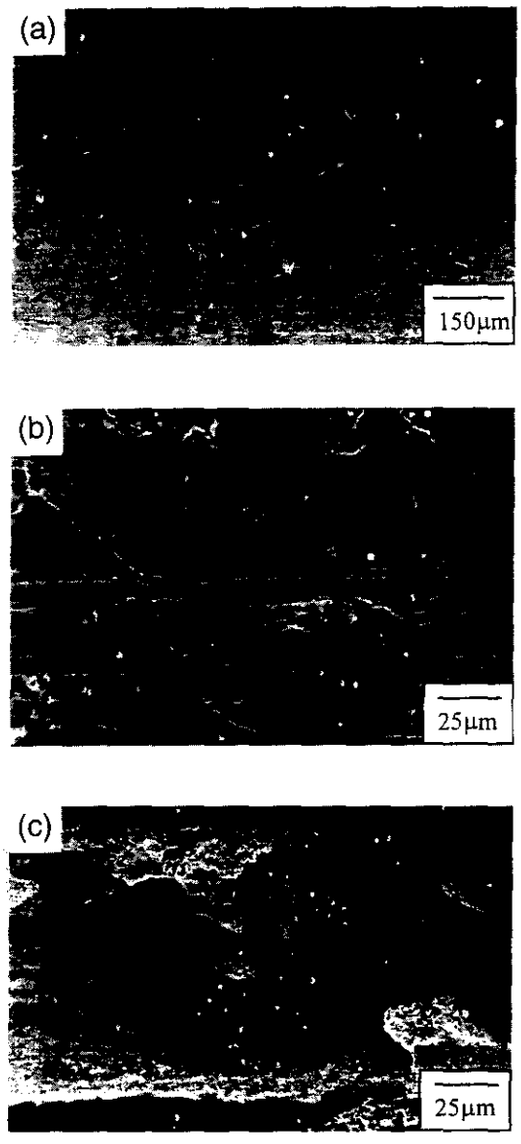

Fig. 8. SEM/SE images of gray cast iron disk tracks after sliding at (a) room temperature, (b) 200°C, and (c) 600°C. Sliding direction of opposite surface is from left to right.

surface. The oxidized-metal nature of this adherent tribolayer is confirmed by the EDS spectra of pin-and-disk worn surfaces and by XRD analysis of the loose wear debris. Direct oxidation of the asperities of the disk surface at flash temperatures can produce the oxidized particles, or they can result from postoxidation of metallic wear debris on the sliding interface.

The main effect of adherent layers of oxidized material on the ceramic pin surfaces is the decrease of the ceramic wear (Fig. 1) by the so-called third-body protection.[34] The thickening of a continuous and relatively homogeneous adherent layer redistributes surface loads and reduces local stresses on the ceramic surfaces.[2] Oxidation wear has been extensively discussed as a main wear mechanism of steel–steel contacts.[23–27,35] However, work in Si_3N_4–iron alloy contacts is comparatively scarce, particularly for sliding above room temperature, where tribooxidation assumes an increasing significance. The works of Kapsa and Viot[13] and Childs and Mimaroglu[14] have investigated the tribological behavior of Si_3N_4 pins against steel disks, in the same temperature range of the present study, 22°–600°C. Gray cast iron has not been the subject of a comparative study. Both papers report that a constant load of 10 N was applied. In the work of Kapsa and Viot,[13] a low-chromium-alloy-bearing steel (DIN N. 1.3505) was tested at a very low sliding speed ($v = 0.5 \times 10^{-3}$ m/s), whereas, in the work of Childs and Mimaroglu,[14] tests were performed at $v = 0.1$ m/s against a tungsten-alloy high-speed steel (DIN N. 1. 3355); these conditions are similar to the present work. Published and present results show an increasing effectiveness of the iron oxide transfers with temperature to protect the nitride surface. Severe disk wear occurs above room temperature, namely, of gray cast iron disks in the present work, as shown in the evolution of K, with temperature (Fig. 4(b)). This sacrificial action of the metallic counterface decreases the values of K with temperature. Oppositely, in the absence of the protective layer, increasing wear with temperature has been reported in Si_3N_4 self-mated pairs.[6,18–21]

The dependence of K on temperature can be examined from a thermodynamic point of view by considering the Arrhenius plots of K_P^{-1} (Fig. 10). Differences of wear rates among SN1, SN2, and SN3 at 100°C and above are not significant within experimental error (Fig. 1). Values of pin wear rate of the three nitride grades were averaged prior to studying the activation energy (Q). The same is true for the disk wear rates of the SN/GCI couples (Fig. 4(b)). The value of the correlation coefficient for the pin wear rates of SN/TS contacts is high; the calculated value of Q is 6.3 kJ/mol. A comparative value of Q for K_P^{-1} in SN/GCI contacts (7.1 kJ/mol) is calculated from the slope of the Arrhenius plot in Fig. 10 for the 100°–600°C temperature range. The way the third body, which is iron oxide-rich, works in protecting the Si_3N_4 surfaces from severe abrasion at temperatures above 100°C is virtually the same for the SN/TS and SN/GCI couples. The values of Q of K_P^{-1} that are calculated for both systems are very similar. The more-abundant and thicker iron oxide layer of the SN/GCI couples (Figs. 7(b)–(d)) enhances the effect of the oxide in improving the wear resistance of the ceramic surface by a factor of 1.5 in comparison to the SN/TS steel; the tool steel is more resistant to oxidation than gray cast iron above 100°C (Fig. 4) because of the chromium.[23,36] The shift of the K_P values to high wear rates observed at room temperature for SN/GCI couples is attributed to the roughness of gray cast iron alloys, as already discussed.

Data of pin wear resistance (K_P^{-1}) in dry sliding of Si_3N_4 (NBD100, Norton, Northboro, MA) against high-speed steel (DIN N. 1. 3355), from the work of Childs and Mimaroglu,[14] has been recalculated, and a single value of $Q = 21.5$ kJ/mol has been obtained in the temperature range 200°–600°C. The temperature dependence of the tribochemical removal rate of Si_3N_4 when polished in chromic acid exhibits an Arrhenius behavior with $Q \approx 20$ kJ/mol.[37] The value of Q of the tribological oxidation of self-mated Si_3N_4 couples in high-temperature and high-pressure water is 21 kJ/mol.[38] This second set of data exhibits an Arrhenius behavior when calculated values of flash temperatures are used for the $1/T$ axis of the Arrhenius plot.[38] In the present study, the Si_3N_4 pins sliding against gray cast iron or tool steel alloys wear less at high temperatures than at room temperature (Fig. 1). The pin wear process has a thermal activation energy that is related to the oxidation wear rate of the metallic counterface. Whereas the tool steel disk wears at a nearly constant rate at and above 100°C (Fig. 4(a)), the continuous increase of the disk wear of gray cast iron (Fig. 4(b)) is a thermally activated process. Metallic disk wear coefficients of SN/GCI couples of the present study and of Si_3N_4/high-speed steel (HSS) couples in the work of Childs and Mimaroglu[14] are plotted in Fig. 11. Net differences in chemical composition and structure of the two iron alloys have not changed the tribooxidation mechanism of the disks. The value of Q of the wear mechanism of the gray cast iron disks (13.7 kJ/mol) for $T \leq 400$°C closely matches the corresponding value of the HSS disk (11.7 kJ/mol) for $T \leq 500$°C. Within the experimental error, gray cast iron disks wear 1.5 times faster than the harder steel disks.

Quinn[23–25,27] has extensively discussed the oxidation wear of alloyed steels due to frictional heating or heat of externa

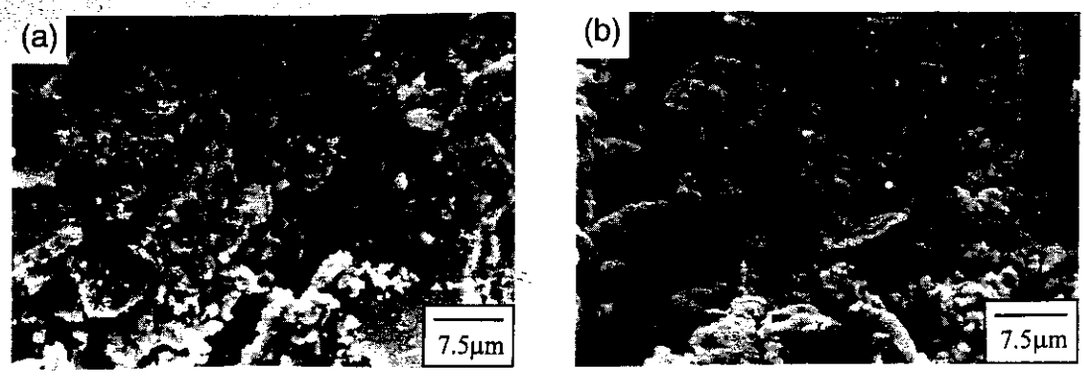

Fig. 9. Morphology of loose wear debris from SN/TS sliding pairs at (a) room temperature and (b) 600°C.

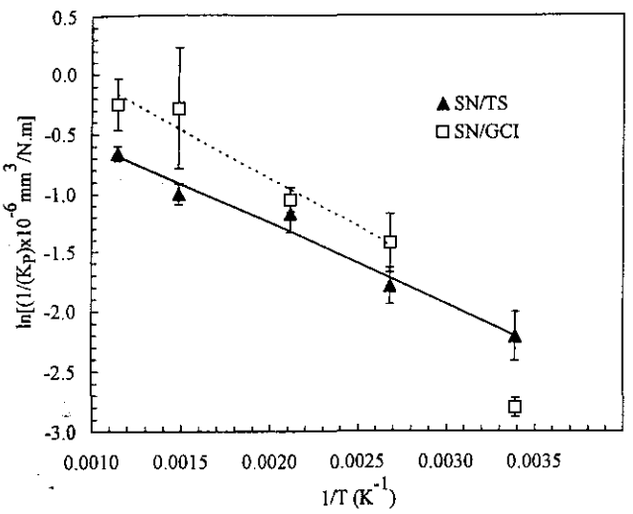

Fig. 10. Arrhenius plots of K_P^{-1} from Si_3N_4 pins sliding against tool steel (TS) and gray cast iron (GCI) disks.

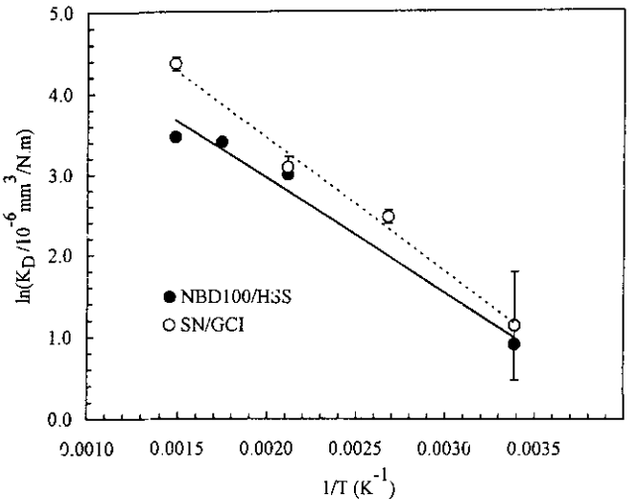

Fig. 11. Arrhenius plots of disk wear coefficients of metallic disks (K_D) sliding against Si_3N_4 pins, from the present experiments with gray cast iron (GCI) and from the literature with high speed steel (HSS).[14]

sources. Tribooxidation activation energies differ from room-temperature testing, where Q = 11.8 kJ/mol for mild-oxidation wear and Q = 7.3 kJ/mol for severe-oxidation wear,[23] to testing at 400°C, where Q is 44.5–51.5 kJ/mol for mild-oxidation wear, with a net contribution from oxidation of the areas of contact that are momentarily "out-of-contact."[24] The change of hardness with temperature accounts for some of the increase of the wear rate at high temperature.[39,40] The discussion of the significance of tribooxidation activation energies remains open, but values are always much lower than those for oxidation in static conditions, where Q = 208 kJ/mol for FeO, Q = 96 kJ/mol or Q = 138 kJ/mol for Fe_3O_4, and Q = 210 kJ/mol for Fe_2O_3.[25,35] The intensification of the steel oxidation rate under friction can be attributed to the coupling of the following effects: (i) increased ease of diffusion under conditions of stress, in the plastic deformed layer, found in similar stress-induced phenomenon-like cyclic stress-induced corrosion,[41] or indentation creep,[39] which reduces Q values comparative to the Q value of the unstrained material; (ii) contact temperatures that develop between asperity tips, which, for high sliding speeds can be much higher than the ambient temperature, thus promoting oxidation, beyond the increase of environmental temperature;[23,24,27,35,36,38] and (iii) a temperature gradient across the metallic oxide scales.[27,36] The Q value for static oxidation of metallic alloys is determined from experiments at isothermal temperatures. In tribotesting, a temperature gradient is created across the oxide scales with the sliding surface of the oxide tips of the asperities at flash temperatures and the general surface at the bulk or average temperature.[27,35,36] The metal–oxide interface of the oxidation reaction decreases along the temperature gradient toward the cool side. As the thickness of the oxide scale grows, the velocity of the metal–oxide interface slows down more than for the diffusion-controlled reaction, in purely isothermal conditions. The way the temperature and diffusion fields link together to give the time to reach the critical thickness for scale delamination or spallation has not been worked out in the literature.[36] At the sliding speed of 0.5 m/s, the increase of flash temperatures above environmental temperatures for Si_3N_4 couples is ~350°C.[19] When flash temperatures are set 350°C above environmental temperatures, the values of Q become 3 times higher than the experimental values of Q calculated from the slopes of the plots in Figs. 10 and 11. Q = 45 kJ/mol is obtained from disk wear data of SN/GCI couples with estimated flash temperatures that are 350°C above environmental temperatures.

The protective tribolayer also determines the frictional behavior of the tribological system.[13,14,22,36,40] Other authors have found that, for a low-alloyed steel,[13] the increase of f for both iron alloys from room temperature to 100°C (Fig. 6) is due to a roughness effect that results from the presence of adherent material on the ceramic surface at 100°C (Fig. 2(b)). The decrease of f of the SN/TS contacts from 100° to 600°C is analogous to that reported in the literature for Si_3N_4/steel couples (f = 0.94 at 22°C to f = 0.76 at 600°C;[13] f = 0.75 at 22°C to f = 0.45 at 600°C[14]). Such behavior is attributed to the influence of surface temperature on the rheological properties of the tribolayer.[14] The friction decrease that has been observed for SN/GCI contacts for temperatures up to 400°C (Fig. 6) should

be favored by the easy tribooxidation and low hot strength of this iron alloy compared to that of hot working tool steel. However, as temperature further increases to 600°C, the severe destruction of the metallic disk (Fig. 8(c)) and the reaction between SiO_2 and iron oxides yield a third body that is increasingly vitreous,[6] leading to the opposite trend of friction.

V. Conclusions

Unlubricated sliding experiments of Si_3N_4 against iron alloys in the range 22°–600°C have shown that ceramic surfaces are progressively protected by a tribolayer of oxidized wear debris. The spinel oxide Fe_3O_4 and the rhombahedral oxide Fe_2O_3 are the main constituents of this adherent layer that results from compacting of products of direct oxidation of the metallic disk wear track or from the postoxidation of loose metallic particles.

The dominant wear mechanisms for the Si_3N_4 and the metallic surfaces are abrasive polishing and tribooxidation followed by delamination. The latter is more pronounced for the gray cast iron disks, which are the least resistant metallic alloy at high temperature. The sacrificial action of the metallic counterface results in the decrease of the ceramic wear coefficient by almost 1 order of magnitude from room temperature to 600°C. Unlike the reported decreasing wear resistance of self-mated Si_3N_4 pairs at high temperatures, Si_3N_4 ceramics sliding against metallic surfaces show increased performance with increasing temperatures.

The evolution of friction coefficient above room temperature reveals characteristic fluctuations, notably in the range 400°–600°C, which is related to the dynamic process of formation, destruction, and renewal of the adherent tribolayer. At room temperature, where the iron oxidation process is much less pronounced and this layer is absent, the friction coefficient remains nearly constant.

Thermal activation energy of the ceramic wear mechanism is inversely related to the oxidational wear of the metallic counterfaces as far as the calculations of the activation energies of the ceramic wear resistance lead to values (Q of 6.3–7.1 kJ/mol) comparable to those of oxidation wear of gray cast iron (Q of 13.7 kJ/mol) and of steel (Q of 7.3–11.8 kJ/mol). These activation energy values are 1 order of magnitude lower than those of oxidation of iron alloys obtained under static conditions as an effect of the enhancement of the potential energy of the reactions under stress.

References

[1]A. Tucci and L. Esposito, "Microstructure and Tribological Properties of ZrO_2 Ceramics," *Wear*, **172**, 111–19 (1994).

[2]Y. J. He, A. J. Winnubst, D. J. Schipper, P. M. Bakker, A. J. Burggraaf, and H. Verweij, "Friction and Wear Behaviour of Ceramic-Hardened Steel Couples Under Reciprocating Sliding Motion," *Wear*, **184**, 33–43 (1995).

[3]K. H. Lee and K. W. Kim, "Effects of Humidity and Sliding Speed on the Wear Properties of Si_3N_4 Ceramics," *Mater. Sci. Eng. A*, **186**, 185–91 (1994).

[4]L. Zhou, L. Fang, N. X. Wang, and J. E. Zhou, "Unlubricated Sliding Wear Mechanism of Fine Ceramic Si_3N_4 Against High-Chromium Cast Iron," *Tribol. Int.*, **27** [5] 349–57 (1994).

[5]S. R. Srinivasan and P. J. Blau, "Effect of Relative Humidity on Repetitive Impact Behavior of Machined Silicon Nitride," *J. Am. Ceram. Soc.*, **77** [3] 683–88 (1994).

[6]X. Dong and S. Jahanmir, "Wear Transition Diagram for Silicon Nitride," *Wear*, **165**, 169–80 (1993).

[7]J. R. Gomes, A. S. Miranda, R. F. Silva, and J. M. Vieira, "Tribological Properties of AlN–CeO_2–Si_3N_4 Cutting Materials in Unlubricated Sliding Against Tool Steel and Cast Iron," *Mater. Sci. Eng. A*, **209**, 277–86 (1996).

[8]L. Fang, Y. Gao, L. Zhou, and P. Li, "Unlubricated Sliding Wear of Ceramics Against Graphitized Cast Irons," *Wear*, **171**, 129–34 (1994).

[9]P. Andersson and K. Holmberg, "Limitations on the Use of Ceramics in Unlubricated Sliding Applications Due to Transfer Layer Formation," *Wear*, **175**, 1–8 (1994).

[10]A. Ravikiran and B. N. P. Bai, "Influence of Speed on the Tribochemical Reaction Products and the Associated Transitions for the Dry Sliding of Silicon Nitride Against Steel," *J. Am. Ceram. Soc.*, **78** [11] 3025–32 (1995).

[11]M. G. Gee and D. Butterfield, "The Combined Effect of Speed and Humidity on the Wear and Friction of Silicon Nitride," *Wear*, **162–164**, 234–45 (1993).

[12]H. Czichos, S. Becker, and J. Lexow, "International Multilaboratory Sliding Wear Tests with Ceramics and Steel," *Wear*, **135**, 171–91 (1989).

[13]P. Kapsa and J. F Viot, "Frottement à Sec de Couples Acier/céramique: Phénomènes Importants," *Rev. Int. Hautes Temp. Refract.*, **21**, 47–61 (1984).

[14]T. H. C. Childs and A. Mimaroglu, "Sliding Friction and Wear Up to 600°C of High-Speed Steels and Silicon Nitrides for Gas Turbine Bearings," *Wear*, **162–164**, 890–96 (1993).

[15]S. T. Buljan and S. F. Wayne, "Wear and Design of Ceramic Cutting Tool Materials," *Wear*, **133**, 309–21 (1989).

[16]R. F. Silva, J. M. Gomes, A. S. Miranda, and J. M. Vieira, "Resistance of Si_3N_4 Ceramic Tools to Thermal and Mechanical Loading in Cutting of Iron Alloys," *Wear*, **148**, 69–89 (1991).

[17]M. Woydt, "Materials-Based Concepts for an Oil-Free Engine"; pp. 459–68 in *New Directions in Tribology*. Edited by I. M. Hutchings. Mechanical Engineering Publications, Ltd., London, U.K., 1997.

[18]H. E. Sliney and C. Dellacorte, "The Friction and Wear of Ceramic/Ceramic and Ceramic/Metal Combinations in Sliding Contact," *Lubr. Eng.*, **50** [7] 571–76 (1994).

[19]A. Skopp, M. Woydt, and K.-H. Habig, "Tribological Behavior of Silicon Nitride Materials Under Unlubricated Sliding Between 22°C and 1000°C," *Wear*, **181–183**, 571–80 (1995).

[20]C. Melandri, M. G. Gee, G. de Portu, and S. Guicciardi, "High-Temperature Friction and Wear Testing of Silicon Nitride Ceramics," *Tribol. Int.*, **28** [6] 403–13 (1995).

[21]S. Danyluk, M. McNallan, and D. S. Park, "Friction and Wear of Silicon Nitride Exposed to Moisture at High Temperatures"; pp. 61–77 in *Friction and Wear of Ceramics*. Edited by S. Jahanmir. Marcel Dekker, New York, 1994.

[22]H. Tomizawa and T E. Fisher, "Friction and Wear of Silicon Nitride at 150°C to 800°C," *ASLE Trans.*, **29** [4] 481–88 (1985).

[23]T. F. Quinn, "Oxidational Wear Modelling: Part I," *Wear*, **153**, 179–200 (1992).

[24]T. F. Quinn, "Oxidational Wear Modelling: Part II. The General Theory of Oxidational Wear," *Wear*, **175**, 199–208 (1994).

[25]T. F. Quinn, *Physical Analysis for Tribology*; pp. 291–359. Cambridge University Press, Cambridge, U.K., 1991.

[26]H. So, "The Mechanism of Oxidational Wear," *Wear*, **184**, 161–67 (1995).

[27]T. F. Quinn, "Computational Methods Applied to Oxidational Wear," *Wear*, **199**, 169–80 (1996).

[28]R. F. Silva, A. P. Moreira, J. R. Gomes, A. S. Miranda, and J. M. Vieira, "The Role of Nitrogen in the Intergranular Glass Phase of Si_3N_4 on High-Temperature Applications and Wear," *Mater. Sci. Eng. A*, **168**, 55–59 (1993).

[29]K. Niihara, R. Morena, and D. P. H. Hasselman, "Evaluation of K_{Ic} of Brittle Solids by the Indentation Method with Low Crack-to-Indenter Ratios," *J. Mater. Sci. Lett.*, **1**, 13–16 (1982).

[30]H. Liu, Q. Xue, and L. Lin, "Wear Maps of TZP/Steel Reciprocating Sliding Couple Under Dry Sliding," *Wear*, **198**, 185–91 (1996).

[31]P. Gautier and K. Kato, "Wear Mechanisms of Silicon Nitride, Partially Stabilized Zirconia, and Alumina in Unlubricated Sliding Against Steel," *Wear*, **162–164**, 305–13 (1993).

[32]M. Terheci, R. R. Manory, and J. H. Hensler, "The Friction and Wear of Automotive Gray Cast Iron Under Dry Sliding Conditions—Part 2. Friction and Wear—Particle Generation Mechanisms and Their Progress with Time," *Wear*, **185**, 119–24 (1995).

[33]Powder Diffraction File. International Centre for Diffraction Data. Newtown Square, PA, 1995.

[34]M. Godet, "Third-Bodies in Tribology," *Wear*, **136**, 29–45 (1990).

[35]S. C. Lim and M. F. Ashby, "Overview n.55. Wear Mechanism Maps," *Acta Metall.*, **35** [1] 1–24 (1987).

[36]F. H. Stott, "The Influence of Oxidation on the Wear of Metals and Alloys"; pp. 391–401 in *New Directions in Tribology*. Edited by I. M. Hutchings. Mechanical Engineering Publications, Ltd., London, U.K., 1997.

[37]T. E. Fisher, "Tribochemistry of Ceramics: Science and Applications"; see Ref. 36, pp. 211–15.

[38]S. Kitaoka, "Tribochemical Wear Theory of Non-Oxide Ceramics in High-Temperature and High-Pressure Water," *Wear*, **205**, 40–46 (1997).

[39]R. F. Silva and J. M. Vieira, "Cutting Performance and Hot Hardness of Si_3N_4-Based Ceramic Inserts," *J. Hard Mater.*, **3** [1] 63–72 (1992).

[40]D. S. Park, "Friction and Wear Measurements of Si_3N_4 at Elevated Temperatures in Air, Ar, and Humid Environments"; pp. 159–80 in *Proceedings of Symposium on Corrosion and Corrosive Degradation of Ceramics*. Edited by R. E. Tressler and M. I. McNallan. American Ceramic Society, Westerville, OH, 1990.

[41]P. J. Bania and S. D. Antolovich, "Activation Energy Dependence on Stress Intensity in Stress-Corrosion Cracking and Corrosion Fatigue"; pp. 157–75 in *Stress Corrosion—New Approaches*. American Society for Testing and Materials, West Conshohocken, PA, 1976. □